Marine and Petroleum Geology 28 (2011) 966–972

Contents lists available at ScienceDirect

Marine and Petroleum Geology

journal homepage: www.elsevier.com/locate/marpetgeo

Cover deformation above steep, basement normal faults: Insights from 2D discrete element modeling

Stuart Hardy*

ICREA (Institució Catalana de Recerca i Estudis Avançats) and Facultat de Geologia, Universitat de Barcelona, 08028 Barcelona, Catalonia, Spain

ARTICLE INFO

Article history:
Received 29 June 2010
Received in revised form
2 November 2010
Accepted 17 November 2010
Available online 24 November 2010

Keywords:
Normal faulting
Reverse faulting
Simulation
Strain

ABSTRACT

A discrete element model is used to investigate progressive cover deformation above a steep (70°), basement normal fault. The cover materials are homogenous with frictional material behavior. In the model shown here both normal and reverse faults in the cover accommodate displacement on the underlying basement fault. The earliest faults are curved, reverse faults which propagate upwards from the basement fault tip into the proto hanging wall. These are replaced, progressively towards the footwall, by subvertical to steep normal faults and finally by a normal fault which dips at an angle predicted by Mohr-Coulomb theory. Thus, most early, secondary structures are located in the hanging-wall of the final, through-going, fault. This structural evolution produces an asymmetric, triangular zone of deformation above the basement fault tip which superficially resembles that associated with trishear; however, its progressive development is quite different. Results also emphasize that the occurrence of reverse faults in extensional settings is not diagnostic of inversion.

1. Introduction

Normal faults are of great importance in crustal evolution in a variety of tectonic settings (e.g., White et al., 1986; Leeder et al., 1991; Gawthorpe et al., 1997; Willsey et al., 2002) with field, laboratory and numerical studies aiding our understanding of their geometry and development (e.g., Vendeville, 1988; McClay, 1990; Withjack et al., 1990; Patton and Fletcher, 1995; Hardy and McClay, 1999; Mandl, 2000; Sharp et al., 2000; Fig. 1a–c). Kinematic models based on inclined shear have been widely used to predict their hanging-wall geometries and strain (e.g., White et al., 1986; Withjack and Schlische, 2006). However, experimental and field evidence points to an early structural evolution which is omitted in simple kinematic models and which often leads to complex hanging-wall/footwall geometries and strain distributions (e.g., Horsfield, 1977; Sharp et al., 2000; Jin and Groshong, 2006). In particular, initial deformation above basement normal faults often involves the development of a monocline which is subsequently breached by through-going faults (e.g., Gawthorpe et al., 1997; Jackson et al., 2006; Fig. 1a–c). Such structures are often described as extensional fault-propagation folds (e.g., Hardy and McClay, 1999). Furthermore, curved, reverse faults ('precursors') are a common feature of early cover deformation, particularly above steeper basement faults (e.g., Horsfield, 1977; Jackson et al., 2006; Fig. 1a and b), although these are sometimes interpreted as evidence for inversion (e.g., Knott et al., 1995). More recently, the trishear kinematic model has been applied to such structures; it predicts observed monocline geometries and zones of potential reverse faulting with some success (e.g., Allmendinger, 1998; Hardy and McClay, 1999; Jin and Groshong, 2006). However, trishear, like many other numerical models, only predicts large-scale fold geometries and bulk strain; it does not reproduce the secondary structures, particularly faults, seen in the field or laboratory. In contrast, discrete element models can replicate both the smaller scale structures seen in the field and laboratory, whilst allowing a detailed analysis of kinematics and strain (e.g., Saltzer and Pollard, 1992; Hardy, 2008). They have been previously used by Finch et al. (2004) and Egholm et al. (2007) to examine deformation above basement normal faults; however Finch et al. did not consider frictional materials in their models, whereas Egholm et al. did not consider deformation above steep (>=65° dip) faults. Here, I build on these studies by using a 2D discrete element model to examine deformation in frictional covers above steep (>=65° dip), basement-involved normal faults. In the model presented here, cover deformation is monitored through its geometric expression, and the incremental shear strain and displacement fields. Results show a structural evolution which begins with the development of steep, reverse faults originating at the basement fault tip and which propagate into the proto hanging-wall: these faults could be

---

* Corresponding author.
E-mail address: stuart.hardy@icrea.es.

0264-8172/$ – see front matter © 2010 Elsevier Ltd. All rights reserved.
doi:10.1016/j.marpetgeo.2010.11.005

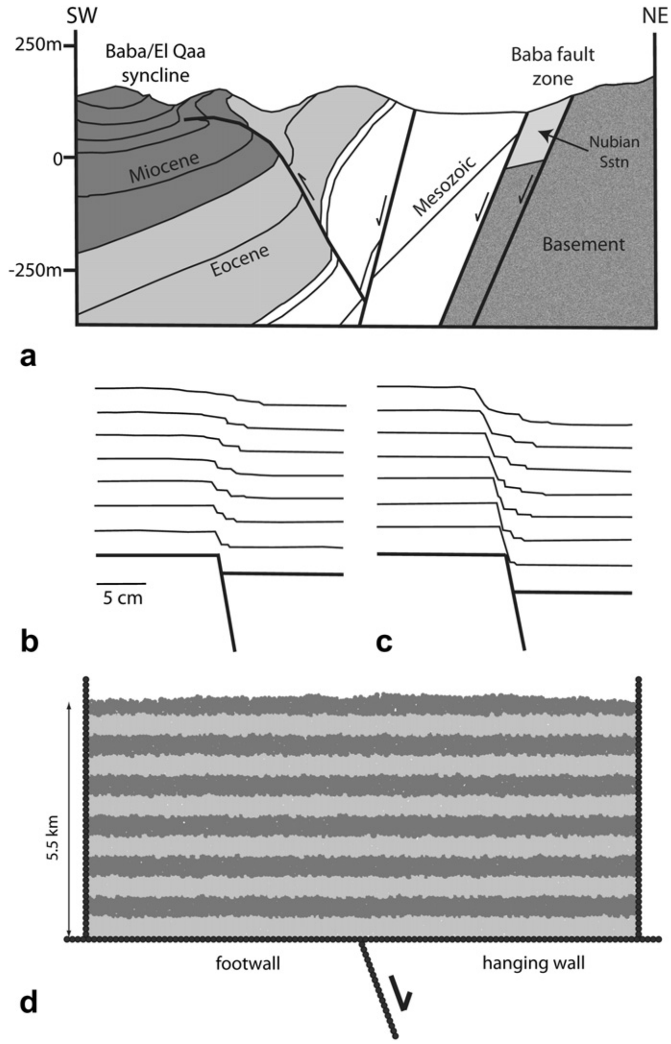

Figure 1. (a–c) Examples of extensional faults from field and analogue models: (a) simplified cross-section across south Wadi Baba showing faulted monocline, major normal faults and secondary reverse faults developed in the hanging-wall of the Baba fault zone, redrawn from Sharp et al. (2000), (b, c) line drawings of progressive deformation above an 80° normal fault in a sandbox analogue model, redrawn from Horsfield (1977), and, (d) discrete element model setup showing initial conditions. See text for discussion.

misinterpreted as evidence for post-rift inversion. These reverse faults are replaced by younger faults that migrate through vertical towards the footwall before finally being replaced by a master, normal fault dipping at an angle expected from Mohr-Coulomb theory (cf. Mandl, 2000). This structural evolution produces a triangular zone of deformation which superficially resembles trishear; however its progressive development is quite different. Implications for the interpretation of hanging-wall deformation in such structures, and the application of kinematic models to them, are discussed.

2. Modeling methodology and boundary conditions

I have conducted a series of discrete element numerical experiments to better understand deformation in a frictional cover (an often-used proxy for the brittle upper crust: eg., Horsfield, 1977; Saltzer and Pollard, 1992), subject to boundary conditions which simulate deformation above steep, normal faults in rigid basement. Modeling of cover deformation to high strain is an ideal candidate for the application of the discrete element technique as it is well-suited to studying problems in which discontinuities (shear-zones, faults, etc) are important as it allows deformation involving unlimited relative motion of individual elements and complex, abrupt boundary conditions (Cundall and Strack, 1979; Finch et al., 2004; Egholm et al., 2007; Hardy, 2008).

The scaled 2D numerical experiments reported here consider a 5.5 by 12.5 km section of the upper crust, subject to displacement on a basement, normal fault centrally located at its base (Fig. 1d). Many different steep fault dips ($\geq 65^\circ$ dip) were investigated, the 70° experiment discussed below is representative of the structural evolution typically observed. Models with a basement fault dip of less than c. 65° typically did not show the development of reverse faults in their early stages of evolution (cf. Horsfield, 1977). The model represents the cover as a densely packed assemblage of c. 12,000 variably sized, circular elements. These elements obey Newton's equations of motion and interact with normal and shear (Mohr-Coulomb) contact forces under the influence of gravity (see Hardy et al., 2009 for a full description of the modeling approach). Element radii range from 25 to 62.5 m, their density is 2500 kg/m^3 and the bulk coefficient of friction (μ) of the modeled body is c. 0.65 giving an internal angle of friction ($\o$) of c. 33°. The cohesion (C) of the assemblage is c. 1 MPa, a value lying within the range of cohesion for natural rock masses (cf. Schultz, 1996). The elastic spring constant used in the calculation of normal and shear forces is $5.5. \times 10^9$ N/m. These parameter values are considered realistic and have been used previously in several discrete element studies in different tectonic settings (cf. Hardy, 2008; Hardy et al., 2009). Displacement on the basement fault is incremented at 0.0025 m per time-step for 600,000 time-steps to achieve a total of 1.5 km. The cover thickness, fault dip and total displacement are similar to those reported from major normal faults in natural settings, e.g. the Gulf of Suez (cf. Gawthorpe et al., 1997). The elements are advanced to their new positions within the model by integrating their equations of motion using Newtonian physics and a velocity-Verlat based numerical scheme (cf. Mora and Place, 1993). Element positions are saved throughout experiments for a detailed, high-resolution analysis of strain history using the program SSPX (Cardozo and Allmendinger, 2009).

3. Simulation results

I illustrate progressive cover deformation in an experiment with a 70° basement fault through its geometric expression and an analysis of incremental shear strain and displacement magnitude (calculated over the preceding 125 m of displacement on the basement fault) (Figs. 2 and 3).

From the geometry and incremental shear strain (Fig. 2), it can be seen that after the initial 125 m of displacement a gentle monocline has developed: there is no visible faulting in the cover (Fig. 2a). Shear strain is localized immediately above the basement fault tip and is diffuse in the rest of the cover; the displacement magnitude field is smooth, fanlike and radiates from the basement fault tip (Fig. 3a). After 250 m displacement a complex zone of steep, curved reverse faults has developed (R) which nucleates at the basement fault tip and has propagated upwards, curving into the hanging-wall (Fig. 2b). This zone of faulting is composed of a single fault at depth, whilst nearer the surface it splays into several minor faults; at the surface the gentle monocline is essentially intact (Fig. 2b). With continued displacement (375 m total), deformation within the fault zone is localized onto a more discrete, subvertical reverse fault (Fig. 2c) which appears to cut much of the cover. The displacement field is now much more partitioned, with discrete jumps in magnitude marking zones of active faulting (Fig. 3c). The next increment of displacement (500 m total), leads to the development of two